PEPPo: Highly Polarized Positrons using MeV Energy Polarized Electrons

J. Grames*, Y. Furletova, J. Guo, F. Lin, V. Morozov, and Y. Zhang
Thomas Jefferson National Accelerator Facility, Newport News, VA 23606, USA

F. Selim
Bowling Green State Universitry, Bowling Green, OH 43403, USA

E. Voutier*
IPN, Université Paris-Sud & Université Paris-Saclay, CNRS/IN2P3, 91406 Orsay, France
(*on behalf of the PEPPo Collaboration)

Motivation for physics with GeV positron beams is described in the context of the 12 GeV Continuous Electron Beam Accelerator Facility (CEBAF), the proposed medium energy Jefferson Lab Electron Ion Collider (JLEIC), as well as for lower energy materials science applications. This motivation is inspired by results of the Polarized Electrons for Polarized Positrons (PEPPo) experiment performed at the CEBAF injector where for the first time the efficient transfer of polarization from electrons to positrons has been demonstrated; positrons produced by the polarized bremsstrahlung radiation induced by an 8.19 MeV/c polarized electron beam in a tungsten target yielded positron polarization measured up to 82%, limited only by the electron beam polarization. Highlights of a proposal to develop a compact high-intensity and high-polarization continuous-wave (cw) polarized positron injector based on the PEPPo method are presented.

PHYSICS MOTIVATION

Positron beams, both polarized and unpolarized, with energies ranging from a few eV to hundreds of GeV are unique tools for the study of the physical world. For energies up to several hundred keV, they allow the study of surface magnetization properties of materials [1] and their inner structural defects [2]. In the several to tens of GeV energy range, they provide the complementary experimental observables essential for an unambiguous determination of the structure of the nucleon [3]. In the several hundreds of GeV energy range, they are considered essential for the next generation of experiments that will search for physics beyond the Standard Model [4].

Physics Interest in CEBAF

In the energy range currently available at JLab, there is no specific difference with respect to the scientific information obtained with an electron or positron probe. However, when more than one quantum electrodynamics based mechanism contributes to a reaction process, the comparison between lepton beams of opposite charge allows one to uniquely distinguish the quantum interference between these mechanisms. This feature is expressed in several key questions about the nucleon structure [3]. The comparison between polarized and unpolarized electrons and positrons is the only experimental technique to single-out effects of two-photon exchange mechanisms, suggested to be responsible for the disagreement between the cross section and polarization transfer measurements of the electric form factor of a proton [5, 6]. Nucleon tomography through generalized parton distributions would also strongly benefit from polarized positron beam capabilities providing a clear experimental path to isolate the interference contributions between the known Bethe-Heitler and unknown virtual Compton amplitudes [7].

Electromagnetic interactions with a polarized positron beam would provide new possibilities to probe the existence of physics beyond the Standard Model, complementary to polarized electron beam techniques. The comparison between a left-handed electron beam and a right-handed positron beam would provide the first measurement of the effective electron-quark coupling quantifying charge-conjugation violation [8]. Positron annihilation also appears as a promising channel in search of a U-boson or heavy photon, a candidate for a Standard Model Dark Matter interaction mediator [9].

Physics Interest in an Electron-Ion Collider

Similarly to the physics motivations of electron-ion collisions, there is an interest in positron-ion collisions at a future Electron-Ion Collider (EIC). A high-intensity polarized positron beam at an EIC could offer an additional probe to study the substructure of nucleons and nuclei. For instance, with polarized electron and positron beams at an EIC one could obtain the full flavor decomposition of the nucleon quark and antiquark distributions, as well as provide understanding of the meson cloud effects and diffractive contributions to structure functions [10]. The flavor separation of the pion and kaon structure could be achieved by comparing the difference between electron and positron interactions involving the Sullivan process [11] with neutral and charged currents. Note that the availability of positron beams may be the only way to get to quark flavor decomposition of the pion and kaon structure, and allow comparisons of the quark and gluon distributions in the pion, kaon and proton.

For a given lepton charge the difference in the left- and right-hand polarized neutral current cross sections is sensitive to the γZ vector interference $F_2{}^{\gamma Z}$ structure function, as well as to the axial vector $xF_3{}^{\gamma Z}$ and $xF_3{}^{Z}$ structure functions. The xF_3 nucleon structure function, for example, which is charge-conjugation odd and mostly dominated by the γZ interference contribution, will be directly sensitive to valence quark distributions [12, 13].

The charged-current deep inelastic scattering (DIS) cross section measurements provide possibly the most direct information on the flavor dependence of quark and antiquark distributions. Depending on the charge of the exchanged W boson, the charged current process will be sensitive to either up-type or down-type flavors. Furthermore, charm and anti-charm production in charged current DIS offers the best way to obtain information on strangeness in the nucleon, and the availability of polarized positron and electron beams would provide the necessary tools to extract strange and anti-strange distributions unambiguously [14, 15]. A high luminosity is essential to perform these measurements.

In addition, the charged current DIS measurements may provide new possibilities to probe for physics beyond the Standard Model. The Standard Model does not predict right-handed charged currents, so that the cross section for electron (positron)-proton charged current DIS with helicity +1(-1) is expected to vanish. Measuring the beam longitudinal polarization sensitivity of the total charged current cross section allows one to set limits on the right-handed W-boson exchange. This requires polarization measurements with high precision [16]. A longitudinally polarized positron beam also offers sensitivity, for example, to squark production in R-parity violating SUSY models, where only left- (right-) handed electrons (positrons) contribute. For leptoquark searches, different lepton beams and polarizations will allow selective increase in the sensitivity to different leptoquark types.

Physics Interest in Low Energy Application

The revolution in next generation electronic devices is tied to the development of spintronic devices in which the electron spin as well as its charge is exploited adding more degrees of freedom. This will offer the possibility of new devices that include high speed memory, ultra-low power logic and photonic devices. Moreover, spin based diodes and transistors can be used as quantum bits enabling quantum computing. The big challenge in developing spin based electronics is spin injection and detection. Spin polarization based positron annihilation spectroscopy is an effective tool for spin detection and for investigating spin injection. The development of an intense polarized positron beam would provide tremendous opportunities to advance the field and facilitate the development of spintronic devices.

A spin polarized positron beam can be used to study ferromagnetism at surfaces and interfaces providing an effective method for measuring spin densities. Because of the sensitivity of positron annihilation spectroscopy (PAS) to vacancy type defects, spin polarization based PAS is also expected to reveal the origin of ferromagnetism in diluted magnetic semiconductors (DMS) and diluted magnetic dielectrics (DMD). The need for intense polarized positron beams in many aspects in spintronics cannot be emphasized enough. For example, current induced spin polarization (CISP) plays a vital role in spintronics, however its mechanism is still under intense debate as it is not clear which of the Spin Hall or Rashba effects provides the major contribution in many systems. A spin polarized positron beam is a promising tool for such a study.

POLARIZED ELECTRONS FOR POLARIZED POSITRONS

Unfortunately, the creation of polarized positron beams is especially difficult. Radioactive sources can be used for low energy positrons [17], but the flux is restricted. Storage or damping rings can be used at high energy, taking advantage of the self-polarizing Sokolov-Ternov effect [18], however, this approach is generally not suitable for external beams and continuous wave facilities.

Instead, schemes for polarized positron production at such proposed facilities rely upon the polarization transfer in the e^+e^--pair creation process from circularly polarized photons [19, 20]. Two different techniques to produce the polarized photons have been investigated successfully: the Compton backscattering of polarized laser light from a GeV unpolarized electron beam [21], and the synchrotron radiation produced by a multi-GeV unpolarized electron beam traveling within a helical undulator [22]. Both experiments demonstrated high positron polarization, confirming the efficiency of the pair production process for producing a polarized positron beam. However, these techniques require high energy electron beams and challenging technologies that limit their range of application.

A new approach, which we refer to as the Polarized Electrons for Polarized Positrons (PEPPo) concept [23, 24], has been investigated at the Continuous Electron Beam Accelerator Facility (CEBAF) of the Thomas Jefferson National Accelerator Facility (JLab). Taking advantage of advances in high polarization, high intensity electron sources [25], it exploits the polarized photons generated by the bremsstrahlung radiation of

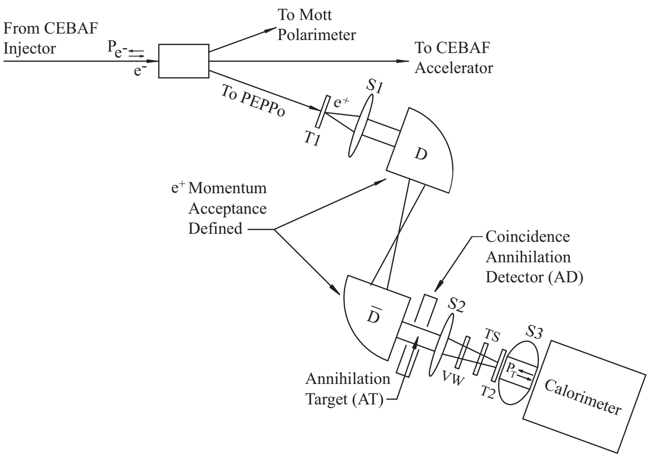

FIG. 1. Schematic of the PEPPo line and apparatus illustrating the principle of operation of the experiment based on the processes sequence $\overrightarrow{e^-} \xrightarrow{T1} \circlearrowleft{\gamma} \xrightarrow{T1} \overrightarrow{e^+} \xrightarrow{T2} \circlearrowleft{\gamma} \xrightarrow{S3} \gamma$ described in the text. The setup footprint is about $3{\times}1.5$ m^2.

low energy longitudinally polarized electrons within a high-Z target to produce polarized e^+e^--pairs. It is expected that the PEPPo concept can be developed efficiently with a low energy (<10 MeV), high intensity (>1 mA), and high polarization (>80%) electron beam driver, opening access to polarized positron beams to a wide community.

PEPPo Experiment at Jefferson Lab

The experiment [26] was designed to evaluate the polarization transfer from a primary electron beam to the produced positrons. A new beam line (Fig. 1) was constructed at the CEBAF injector [27] where polarized electrons up to 8.19 MeV/c were transported to a 1 mm thick tungsten positron production target (T1) followed by a positron collection, selection, and characterization system [28]. Longitudinally polarized electrons interacting in T1 radiate elliptically polarized photons whose circular component (P_γ) is proportional to the electron beam polarization (P_e). Within the same target, the polarized photons produce polarized e^+e^--pairs with perpendicular ($P_\perp$) and longitudinal ($P_\parallel$) polarization components both proportional to P_γ and therefore P_e. The azimuthal symmetry causes $P_\perp$ to vanish resulting in longitudinally polarized secondary positrons. Immediately after T1, a short focal length solenoid (S1) collects the positrons into a combined function spectrometer (D$\overline{\text{D}}$) composed of two 90° dipoles that select positron momentum. The exiting positrons can either be detected at a positron diagnostic (AT+AD) or refocused by a second solenoid (S2) through a vacuum window (VW) to a Compton transmission polarimeter. Retracting T1, the known electron beam was additionally transported to T2 to calibrate the polarimeter analyzing power.

This polarimeter [28] begins with a 2 mm densimet (90.5%W/7%Ni/2.5%Cu) conversion target (T2) followed by a 7.5 cm long, 5 cm diameter iron cylinder centered in a solenoid (S3) that saturates and polarizes it. The average longitudinal polarization was measured to be $\overline{P_T} = 7.06 \pm 0.09\%$, in very good agreement with the previously reported value [28]. An electromagnetic calorimeter with 9 CsI crystals ($6{\times}6{\times}28$ cm^3) arranged in a $3{\times}3$-array is placed at the exit of the polarimeter solenoid. Polarized positrons convert at T2 via bremsstrahlung and annihilation processes into polarized photons with polarization orientation and magnitude that depend on the positron polarization. Because of the polarization dependence of the Compton process, the number of photons passing through the iron core and subsequently detected by the CsI-array depends on the relative orientation of the photon and iron core polarizations. By reversing the sign of the positron polarization (via the electron beam helicity) or the target polarization (via S3 polarity), one measures the experimental Compton asymmetry

$$A_C^p = P_\parallel \, \overline{P_T} \, A_p = \epsilon_P \, P_e \, \overline{P_T} \, A_p \tag{1}$$

where A_p is the positron analyzing power of the polarimeter and ϵ_P is the electron-to-positron polarization transfer efficiency. Knowing P_T, P_e, A_p and measuring A_C^p provide a measurement of $P_\parallel$ and ϵ_P.

PEPPo used a polarized electron beam of p_e=8.19±0.04 MeV/c to measure the momentum dependence of ϵ_P over the positron momentum range of 3.07 to 6.25 MeV/c. The magnetic beam line and polarimeter were first calibrated using electron beams of precisely measured polarization and with momenta adjusted to match the positron momenta to be studied. Only the polarity of the spectrometer was reversed when measuring positrons instead of electrons. The experimental values of S1, D$\overline{\text{D}}$, and S2 currents agree well with those determined by a GEANT4 [29] model of the experiment using magnetic fields modeled with OPERA-3D [30].

The polarization of the electron beam, P_e, was measured to be 85.2±0.6±0.7% with a Mott polarimeter [31]. The first uncertainty is statistical and the second is the total systematic uncertainty associated with the theoretical and experimental determination of the Mott analyzing power.

The AD diagnostic is used to demonstrate the presence of positrons exiting the D$\overline{\text{D}}$ spectrometer. When interacting with an insertable chromium oxide target (AT in Fig. 1) at the spectrometer exit, positrons annihilate into two back-to-back 511 keV photons (Fig. 2) that are detected by a pair of NaI detectors (AD in Fig. 1).

The PEPPo beam line, magnet fields, and detection system was modeled using GEANT4, taking advantage of a previous implementation of polarized electromagnetic processes [32, 33]. The calibration of the analyzing power of the polarimeter relies on the comparison between experimental and simulated electron asymmetries. It allowed us to benchmark the GEANT4 physics packages and resolve related systematic uncertainties within the limits of the measurement accuracy. Details of the electron analyzing power calibration and computation of the positron analyzing power may be found in [26].

PEPPo Results

The positron longitudinal polarization $P_{\parallel}$ and the polarization transfer efficiency ϵ_P as obtained from Eq. 1 are reported in Fig. 3. These data show large positron polarization ($P_{\parallel} > 40\%$) and polarization transfer efficiency ($\epsilon_P > 50\%$) over the explored momentum range. The bremsstrahlung of longitudinally polarized electrons is therefore demonstrated as an efficient process to generate longitudinally polarized positrons. The e^+ production efficiency deduced from the analysis of the photon rates at AD is $\sim 10^{-6}$, in agreement with expectations [34] and optical simulations of the experimental apparatus.

A POLARIZED POSITRON INJECTOR FOR JEFFERSON LAB

While the polarization transfer by bremsstrahlung and pair creation is similarly efficient for any incident electron energy, the yield of positrons is not. Rather, the positron yield scales approximately with the incident electron beam power, thus higher electron beam energy is favorable from this perspective. For example, at the Stanford Linear Accelerator Center, a 35 GeV electron beam was used to produce and collect 220 MeV positrons with e^+e^- efficiency of $\sim$1 [35], whereas at the APosS system at Argonne National Laboratory, a 12-20 MeV electron beam was used to produce and collect moderated slow positrons with efficiency of $\sim 10^{-7}$ [36].

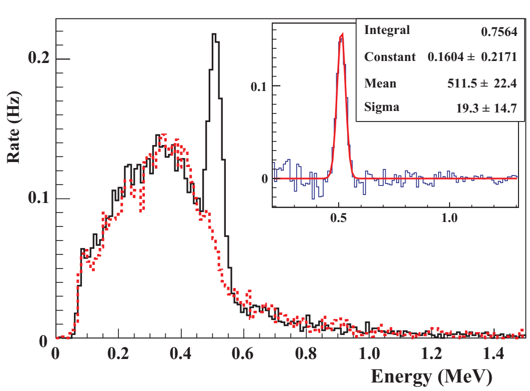

FIG. 2. (Color) Measured energy spectra in one of the annihilation detectors (AD) once T1 is inserted in (full line) or removed from (dash line) the electron beam path; the top right corner shows the difference between these spectra.

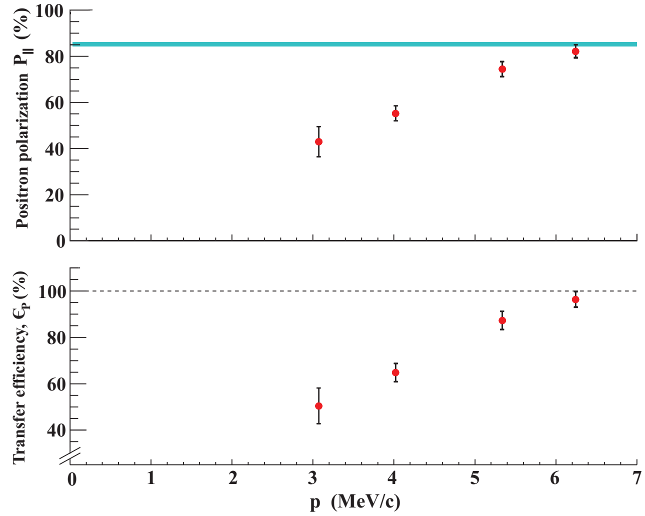

FIG. 3. (Color) PEPPo measurements of the positron polarization (top panel) and polarization transfer efficiency (bottom panel); statistics and systematics are reported for each point, and the shaded area indicates the electron beam polarization.

However, limiting the electron beam energy (< 10 MeV) one may significantly mitigate subsequent radioactivity of the production target and positron collection beam by operating below the photo-neutron production threshold. Consequently, maximizing the polarized electron beam intensity and achieving very efficient collection of the low energy positrons exiting the conversion target are important factors.

In particular, the strategy we propose to satisfy injection into JLEIC is charge accumulation. However, rather than accumulating *hot positrons* after conversion we propose to accumulate *cold electrons* before conversion. A high-level diagram of the polarized positron injector is shown in Fig. 4 along with preliminary parameters at each step along the injector chain. Here, we explain the requirements for polarized positron production for JLEIC [37] experiments assuming a luminosity $\sim 10^{33} cm^{-2} s^{-1}$ and polarization > 40% goals.

Accumulation of polarized positrons in the JLEIC electron collider ring requires an average polarized positron current of about 10 nA, considering a reasonably short injection time and sufficient average injected beam current to maintain high equilibrium polarization. Fig. 5 shows the polarized positron bunch train pattern injected into the JLEIC collider ring. The 17 MHz micro bunch train from the polarized positron injector is common to the fundamental RF frequencies of CEBAF 1497 MHz (1/88 of 1497 MHz) and JLEIC 476 MHz (1/28 of 476 MHz).

Assuming the polarized positron production and collection efficiency measured in PEPPo is improved to e.g. $\sim 10^{-4}$ by optimizing the target material/thickness, providing more efficient collection, and maximizing the figure of merit IP^2, a polarized electron bunch charge of

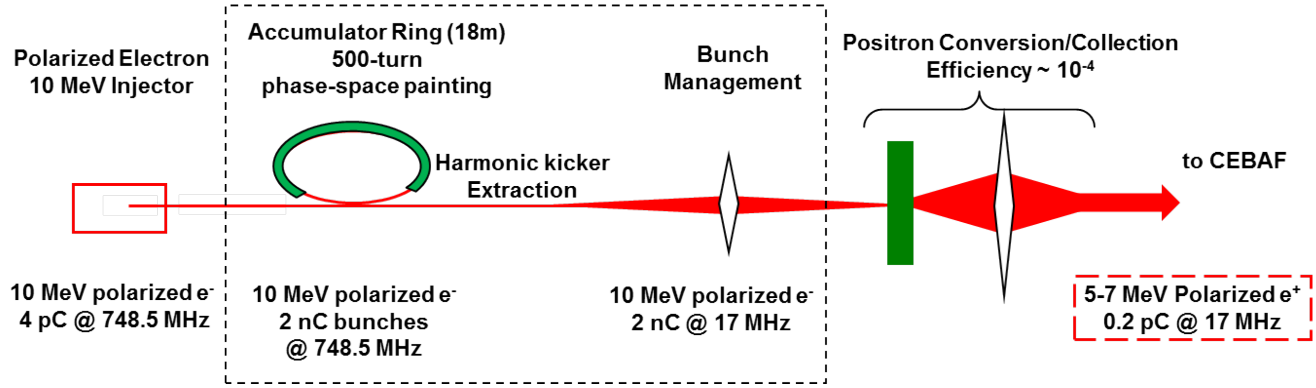

FIG. 4. (Color) 10 MeV polarized electron injector provides bunches that are accumulated 500 turns in an accumulator ring before being extracted to a positron conversion target, where polarized positrons are created and collected to a beam of about 5 MeV.

4 pC at a frequency of 748.5 MHz is required. Such a bunch charge is within the reach of a polarized electron gun. As shown in Fig. 5, the injection into the JLEIC collider ring in a cw fashion is not possible because the injected bunches need on the order of 20 ms to damp to the design orbit. Thus, the key of polarized positron injection into the JLEIC is a positron source that provides a low-duty, relatively high-current micro bunch structure with low average current. As shown in Fig. 4, lowering the duty factor is accomplished by collecting the beam coming from the electron source within an accumulator ring.

A variety of techniques exist that are possible for beam accumulation. Our approach is to demonstrate the phase-space painting as the viable option to pursue. The phase-space painting does not increase the local phase-space density but accumulates the beam at the expense of increasing its 6D emittance. For this reason, accumulating polarized positrons with a low phase-space density would probably not be efficient. On the other hand, electron bunches can be generated at the photo cathode with very low emittances and can be efficiently stacked in the accumulator ring. One may consider using damping rings for accumulation of a few GeV electrons or positrons. However, such damping rings are usually large complicated devices. At low energies of a few MeV, one cannot rely on synchrotron radiation for cooling. Another cooling technique, ionization cooling, even if feasible, results in large equilibrium emittances, which make the beam difficult to use.

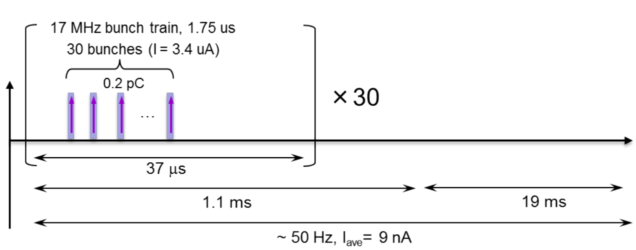

FIG. 5. (Color) Polarized positron bunch injection pattern for the JLEIC electron collider ring.

To produce a desired cw positron beam, one only needs a polarized electron beam with similar electron bunch structure (but higher bunch charge due to the low production and collection efficiency), conversion target and collection system, the components outside of the box indicated in Fig. 4. Beam parameters at each stage of the polarized positron injection scheme that satisfy both the discussed JLEIC and CEBAF physics programs is summarized in Tab. I. R&D activities required to realize the proposed positron injector are described in the following sections.

Polarized Electron Source

GaAs-based photo-guns used at accelerators with extensive user programs must exhibit long photocathode operating lifetimes. Two dc-high voltage GaAs photo-guns have been built at Jefferson Lab based on a compact inverted insulator design [38] and operated using high polarization photocathodes. One photo-gun provides the polarized electron beam at CEBAF with current up to 200 μA. The other photo-gun was used for high average current photocathode lifetime studies at a dedicated test facility up to 4 mA of polarized beam and 10 mA of unpolarized beam. In achieving this the photo-guns employ the best learned practices, e.g. (a) operating with the drive laser beam positioned away from the electrostatic center of the cathode/anode, (b) limiting the photocathode active area to eliminate photoemission by stray light, (c) using a large drive laser beam to distribute ion damage over a larger area, (d) applying low bias voltage to the anode to repel ions downstream of the gun, and (e) operating with immeasurable field emission. However, further gains are necessary in order for sustained operation of the polarized electron source at milliAmpere currents to be realized.

TABLE I. Beam parameters at stages of the polarized positron injection scheme for JLEIC and CEBAF physics programs.

Case	Polarized Electron Source	Accumulator Ring	Electrons at Converter	Polarized Positron Source
JLEIC	4 pC @ 748.5 MHz 3 mA, DF=5%	2 nC @ 748.5 MHz 1.5 A, DF=5%	2 nC @ 17 MHz 34 mA, DF=0.26%	0.2 pC @ 17 MHz 3.4 μA, DF=0.26%
CEBAF	4-40 pC @ 250 MHz 1-10 mA (cw)	Unnecessary	4-40 pC @ 250 MHz 1-10 mA (cw)	0.4-4 fC @ 250 MHz 0.1-1.0 μA

High average current and/or high bunch charge applications benefit from the operation of the photo-gun at very high voltage, which serves to minimize the ill-effects of space charge forces which degrade the emittance and introduce beam loss leading to a diminished photo-gun charge lifetime. Photo-guns with higher high voltage allow for compact, less-complicated injectors. Higher HV would also increase QE by lowering the potential barrier (Schottky effect) [39] and suppresses the surface charge limit [40]. As an added benefit, operation at very high bias voltage may enhance the operating lifetime of the photo-gun by quickly accelerating the beam to energy with very small ionization cross section. The total number of ions generated at 500 kV, for example, will be substantially reduced compared to operation at 100 kV, assuming the same cathode/anode gap, see Fig. 6.

A number of photo-gun groups are working to build 500 kV guns, however without exception efforts to operate photo-guns at 500 kV and maximum field strength greater than 10 MV/m have met with problems due to field emission. At Jefferson Lab, a new photo-gun is being constructed that will employ proven vacuum techniques such as pre-baking at 400°C to reduce outgassing, as well as cryo-pumping if ongoing vacuum tests indicate an improvement over conventional pumping with NEGs and ion pumps. The adjoining beam line will be properly engineered for $\sim 10^{-12}$ Torr operation and techniques will be used to minimize the effect of ion bombardment, in particular the use of a larger laser beam spot size at the photocathode. But the main focus of the new photo-gun design effort is directed at operation at high voltage of 500 kV, making use of a longer ceramic insulator and a spherical cathode.

Polarized Electron Accumulator Ring

The main function of the accumulator ring is to convert the high duty factor, low intensity electron bunch train available from the electron gun into low duty factor and high charge per bunch beam, using multi-turn phase painting injection. To match the RF frequency of CEBAF (1497 MHz) and the colliding bunch repetition rate in JLEIC (476 MHz), a 17 MHz (1/88 of 1497 MHz) bunch train needs to be extracted rom the accumulator ring.

The injection system design will be similar to that of the CERN LEIR ring shown in Fig. 7 (left). Multi-turn injection is accomplish through transverse phase-space painting [41]. Using two pairs of bumper magnets, shown in Fig. 7 (right), the orbit is transversely displaced near an electrostatic septum where each subsequent turn is injected. While LEIR has successfully demonstrated 75 turn injection of Pb^{54+} we aim for a more aggressive 500 turn injection to take advantage of the relatively small electron emittance. In the case of 4D transverse phase-space painting, an increase of 30 in the transverse 2D emittance is expected. Ultimately, the emittance must also satisfy the required beam size at the positron production target. Simulation and optimization of the multi-turn injection scheme will be an important component of the final solution.

A harmonic stripline radio-frequency (RF) kicker is considered for use for the accumulator ring extraction. Stripline RF kickers are used widely in beam feedback systems, and also used for beam extraction in storage rings such as KEK-ATF [42]. Stripline kickers have the advantage of short rise/fall times, a critical issue for successful extraction from the accumulator ring extraction. The RF power required for the stripline kicker at low energy beam is additionally affordable. For example, a PEP-II stripline kicker requires 500 W of power in 22 combined harmonics to deflect a 10 MeV beam by 1 mrad for the proposed beam time structure. Commercial broadband amplifiers can achieve rise times in approximately 10 ns.

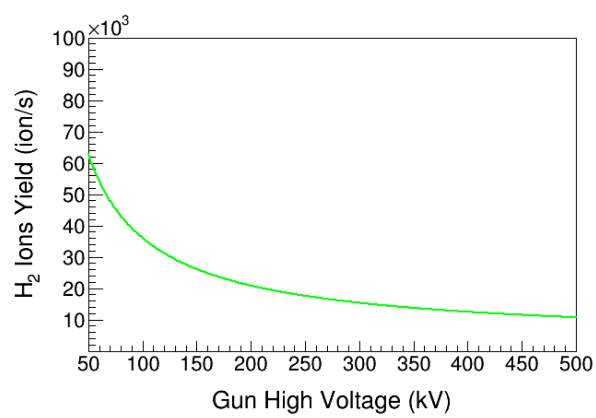

FIG. 6. (Color) Ions yield assuming electron beam current of 2.0 mA and gun vacuum of 8.0 x 10^{-12} Torr.

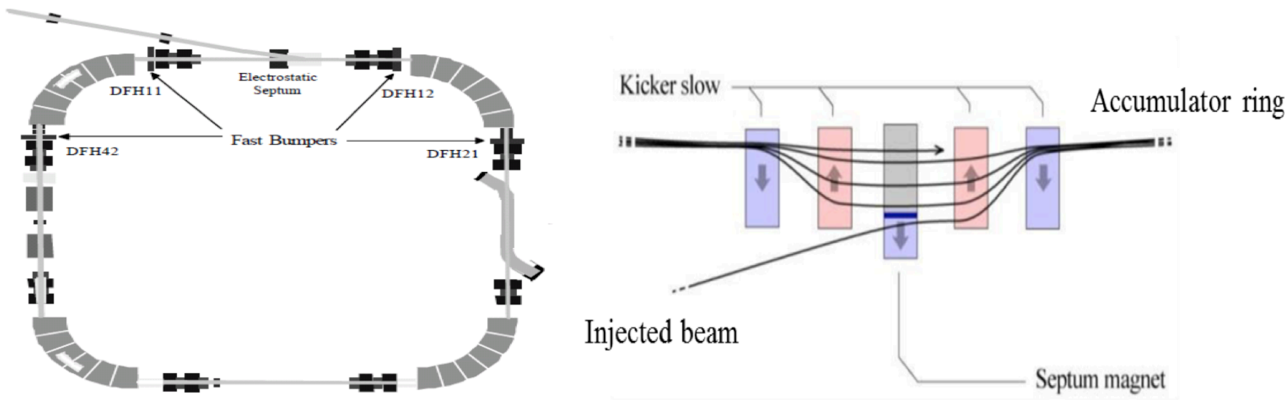

FIG. 7. (Color) Low Energy Ion Ring (LEIR) at CERN (left) and LEIR injection magnets (right).

To preserve the polarization, a full solenoid Siberian snake is placed at the symmetry point $\theta = \pi$ with respect to the injection location in the accumulator ring. The snake rotates the spin by 180° and sets the invariant spin field (spin closed orbit vector) in the horizontal plane. The orientation of invariant spin field depends on the energy and the location in the ring, except the injection location where the spin lies along the axis of the solenoid field, i.e. the longitudinal direction. This guarantees that the injected beam polarization is aligned with the stored beam during accumulation. Simulation of spin dynamics is necessary to successfully demonstrate preservation of the electron polarization.

The accumulator ring may also prove beneficial for the injection of polarized electrons into JLEIC because electron injection similarly requires high-macro-bunch-current low-duty-factor electron trains like that imagined for the positron source concept.

Polarized Positron Source

For any reasonable electron beam size at the production target, the outgoing positron angular spread greatly dominates over the initial electron angular spread. Therefore, the positron emittance in each plane after the target can be written as $\epsilon_{x,y} \approx \sigma_{x,y} \cdot \theta_{x,y}$ where $\sigma_{x,y}$ is the horizontal/vertical electron beam size at the radiator. Minimizing the electron beam size at the radiator lowers the final positron emittance.

However, the power deposition density in such a converter will be extreme, with most of the average power of 10 kW delivered by the 1 mA and 10 MeV electron beam deposited in the target. The design of such a system requires careful considerations on material selection, and on the type of engineering solutions implemented. Rastering could be implemented, but this tends to increase the beam size at the target. Rather, a high power beam absorbers composed of a cooled liquid metal target, like that developed by Niowave Inc., may solves this problem.

The efficient collection of the positrons into a suitable beam for injection into CEBAF is a sophisticated problem requiring many variables to be specified for an optimal solution. Introduced into accelerator physics relatively recently (1992) the Multi-Object Genetic Algorithm (MOGA) is a powerful tool to optimize multi-dimensioned non-linear problems. It has been increasingly employed to optimize the design and operating parameters e.g. at Cornell [43] to achieve a bright high-current electron or to optimize luminosity for the International Linear Collider design [44].

The strength of this technique with respect to the proposed work is the capability to globally judge desirable or dominant traits such as positron yield, beam brightness (yield/emittance), figure of merit (yield x polarization^2), and so on. While some parameters readily optimize (e.g. one may always benefit from an electron drive beam with highest polarization), it is possible with a large parameter base for design-bias or local optimization (meaning, a subset of parameters in the system) to mislead.

SUMMARY

It is expected that the PEPPo concept can be developed efficiently with a low energy (<10 MeV), high intensity (>1 mA), and high polarization (>80%) electron beam driver, opening access to polarized positron beams for a wide community. Proposed R&D activities required to realize a proposed positron injector suitable for a physics program at CEBAF or JLEIC are presented.

This work was supported in part by the U.S. Department of Energy, the French Centre National de la Recherche Scientifique, and the International Linear Collider project. Jefferson Science Associates operates the Thomas Jefferson National Accelerator Facility under DOE contract DE-AC05-06OR23177.

[1] R. W. Gidley, A. R. Köymen, and T. W. Capehart, Phys. Rev. Lett. **49**, 1779 (1982).

[2] R. Krause-Rehberg and H. S. Leipner, *Positron Annihilation in Semi-conductors* (Springer-Verlab Berlin Heidelberg, 1999).

[3] E. Voutier, in *Nuclear Theory*, Vol. 33, edited by A. I. Georgievia and N. Minkov (Heron Press, Sofia, 2014) p. 142.

[4] T. Behnke, J. E. Brau, B. Foster, J. Fuster, M. Harrison, J. M. Paterson, M. Peskin, M. Stanitzki, N. Walker, and H. Yamamoto, *The International Linear Collider Technical Design Report*, Executive summary 1 (2013).

[5] P. Guichon and M. Vanderhaeghen, Phys. Rev. Lett. **91**, 142303 (2003).

[6] P. G. Blunden, W. Melnitchouk, and J. A. Tjon, Phys. Rev. Lett. **91**, 142304 (2003).

[7] M. Diehl, in *Cont. to the CLAS12 European Workshop* (Genova, Italy, 2009).

[8] X. Zheng, AIP Conf. Proc. **1160**, 160 (2009).

[9] B. Wojtsekhowski, AIP Conf. Proc. **1160**, 149 (2009).

[10] A. Accardi *et al.*, Eur. Phys. J. **52**, 268 (2016).

[11] J. R. McKenney, N. Sato, W. Melnitchouk, and C.-R. Ji, Phys. Rev. D **93**, 054011 (2016).

[12] V. Chekelian, in *DIS2010* (PoS, 2010) p. 187.

[13] F. D. Aaron *et al.* (H1 Collaboration), JHEP. **1209**, 061 (2012).

[14] Z. Zhang (H1 Collaboration), in *ICHEP2012* (PoS, 2013) p. 289.

[15] V. Barone, U. D'Alesio, and M. Genovese, hep-ph/9610211.

[16] U. Stoesslein *et al.*, Tech. Rep. ZEUS-05-003.

[17] P. W. Zitzewitz, J. C. V. House, A. Rich, and D. W. Gidley, Phys. Rev. Lett. **43**, 1281 (1979).

[18] A. A. Sokolov and I. M. Ternov, Sov. Phys. Dokl. **8**, 1203 (1964).

[19] H. Olsen and L. Maximon, Phys. Rev. **114**, 887 (1959).

[20] E. A. Kuraev, Y. Bistritskiy, M. Shatnev, and E. Tomasi-Gustafsson, Phys. Rev. C **81**, 055208 (2010).

[21] T. Omori *et al.*, Phys. Rev. Lett. **96**, 114801 (2006).

[22] G. Alexander *et al.*, Phys. Rev. Lett. **100**, 210801 (2008).

[23] E. G. Bessonov and A. A. Mikhailichenko, in *EPAC96* (JACoW, 1996) p. THP071L.

[24] A. P. Potylitsin, Nucl. Inst. Meth. A **398**, 395 (1997).

[25] P. Adderley *et al.*, Phys. Rev. ST Acc. Beams **13**, 010101 (2010).

[26] D. Abbott, P. Adderley, A. Adeyemi, P. Aguilera, M. Ali, H. Areti, M. Baylac, J. Benesch, G. Bosson, B. Cade, A. Camsonne, L. S. Cardman, J. Clark, P. Cole, S. Covert, C. Cuevas, O. Dadoun, D. Dale, H. Dong, J. Dumas, E. Fanchini, T. Forest, E. Forman, A. Freyberger, E. Froidefond, S. Golge, J. Grames, P. Guèye, J. Hansknecht, P. Harrell, J. Hoskins, C. Hyde, B. Josey, R. Kazimi, Y. Kim, D. Machie, K. Mahoney, R. Mammei, M. Marton, J. McCarter, M. McCaughan, M. McHugh, D. McNulty, K. E. Mesick, T. Michaelides, R. Michaels, B. Moffit, D. Moser, C. Muñoz Camacho, J.-F. Muraz, A. Opper, M. Poelker, J.-S. Réal, L. Richardson, S. Setiniyaz, M. Stutzman, R. Suleiman, C. Tennant, C. Tsai, D. Turner, M. Ungaro, A. Variola, E. Voutier, Y. Wang, and Y. Zhang (PEPPo Collaboration), Phys. Rev. Lett. **116**, 214801 (2016).

[27] R. Kazimi *et al.*, in *EPAC04* (JACoW, 2004) p. TUPLT164.

[28] G. Alexander *et al.*, Nucl. Inst. Meth. A **610**, 451 (2009).

[29] S. Agostinelli *et al.*, Nucl. Inst. Meth. A **506**, 250 (2003).

[30] J. Benesch, *Modeling of the PEPPo spectrometer*, PEPPo **TN-15-07** (Jefferson Laboratory, Newport News, Virginia, 2015).

[31] J. Grames *et al.*, in *PSTP13* (PoS, 2013) p. 040.

[32] R. Dollan, K. Laihem, and A. Schälicke, Nucl. Inst. Meth. A **559**, 185 (2006).

[33] J. Dumas, J. Grames, and E. Voutier, AIP Conf. Proc. **1160**, 120 (2009).

[34] J. Grames, E. Voutier, *et al.*, *Polarized electrons for polarized positrons: a proof-of-principle experiment*, Experiment **E12-11-105** (Jefferson Laboratory, Newport News, Virginia, 2011).

[35] J. Clendenin, *High-Yield Positron Systems for Linear Colliders*, Tech. Rep. SLAC-PUB-4743 (SLAC, 1989).

[36] C. Jonah, Applied Surface Science **255**, 25 (2008).

[37] S. Abeyratne *et al.*, *MEIC Design Summary*, Tech. Rep. (Jefferson Laboratory, Newport News, Virginia, 2015) arXiv:1504.07961.

[38] R. Suleiman, P. Adderley, J. Clark, S. Covert, J. Grames, J. Hansknecht, M.Poelker, and M. Stutzman, in *Electron Ion Collider Workshop* (Jefferson Lab, 2014).

[39] J. R. Howorth *et al.*, Applied Physics Letters **23**, 123 (1973).

[40] G. A. Mulhollan *et al.*, Physics Letters A **282**, 309 (2001).

[41] A. Fowler and K. D. Metzmacher, CERN-PS-CA-Note-98-22-Tech (1998).

[42] T. Naito *et al.*, in *EPAC08* (Genoa, Italy, 2008) MOPP025.

[43] I. V. Bazarov and C. K. Sinclair, Physical Review Accelerators and Beams **8**, 034202 (2005).

[44] I. V. Bazarov and H. Padamsee, in *Proceedings of the 2005 Particle Accelerator Conference* (IEEE 0-7803-8859-3, 2005) pp. 2188–2190.